162. Transition Metal Complexes with Bidentate Ligands Spanning *trans*-Positions. XII.[1]) Steric Effects in the Kinetics and Mechanism of Substitutions at Hydride and Methyl Bisphosphine Platinum (II) Complexes

by **Lars I. Elding**

Physical Chemistry 1, Chemical Center, University of Lund, P.O. Box 740, S-22007 Lund

and **Bruno Kellenberger** and **Luigi M. Venanzi***

Laboratorium für Anorganische Chemie, ETH-Zentrum, Universitätstrasse 6, CH-8092 Zürich

(16.V.83)

Summary

Ligand substitution reactions on square-planar platinum(II) complexes of the types *trans*-[PtRXL$_2$], *trans*-[PtR(4-PADA)L$_2$][BF$_4$], *trans*-[PtRX($\widehat{L}$L)] and *trans*-[PtR(4-PADA)($\widehat{L}$L)][BF$_4$] (R = H, Me; X = Cl$^-$, I$^-$; L = PEt$_3$, bis(3-trifluoromethylphenyl)benzylphosphine (**4**), $\widehat{L}$L = the *trans*-spanning 2,11-bis[bis(3-trifluoromethylphenyl)phosphinomethyl]benzo[*c*]phenanthrene (**3**); 4-PADA (= pyridine-4-azo-4′-(*N*, *N*-dimethyl)aniline) have been studied at 30° using stopped-flow and conventional spectrophotometry, methanol as solvent, and 2.5×10^{-2} M ionic strength ($LiClO_4$ as supporting electrolyte). 4-PADA was used as indicator ligand, as its absorption spectrum differs from those spectra where it is complexed.

The expected steric effects of the bulky ligands, especially of **3**, on the rates and mechanisms of all the reactions studied are small. All reactions take place by the usual two-term rate law. Noteworthy, for the complexes with the bulky ligands **3** and **4**, the direct reaction path with the entering nucleophile is predominant. There is no preference for a solvent or dissociative path. The reactivity order for the hydride complexes is *trans*-[PtHX(PEt$_3$)$_2$] < *trans*-[PtHX(**4**)$_2$] < *trans*-[PtHX(**3**)]. However, for the corresponding methyl complexes, there is some retardation by ligand **3**, probably due to an interaction between the methyl group and the hydrocarbon moiety of **3**, which inhibits the fluxional behavior of this ligand. The results have some relevance for the understanding of olefin-insertion reactions of hydride complexes containing these phosphine ligands.

1. Introduction. – The coordination chemistry of the bidentate ligand 2,11-bis(diphenylphosphinomethyl)benzo[*c*]phenanthrene (**1**), has been extensively

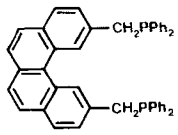

1

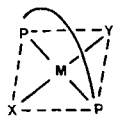

2

[1]) Part XI (erroneously denoted as Part XII): see [1].

studied [1] as it was believed [2] that this ligand would induce the preferential formation of square planar complexes of type **2** with a wide variety of metal centers. The use of this ligand does indeed result in the preferential formation of complexes in which the P-M-P bond-angle is *ca.* 180°. Thus, the complexes $[NiX_2(\mathbf{1})]$ (X = Cl, Br and I) are of type **2** in the solid state and in solution [3] while the corresponding monodentate complexes $[NiX_2\{PPh_2(CH_2Ph)\}_2]$ can be obtained either as square planar or pseudo-tetrahedral species in the solid state and as mixtures of the two forms in solution [4]. Furthermore, while the P-Au-P bond angle in $[AuCl(\mathbf{1})]$ is 175.7 (1)° [5], it is only 132.1 (1)° in $[AuCl(PPh_3)_2]$ [6].

However, this preference for the formation of complexes with nearly linear P-M-P geometries is not very marked. Thus, $[CoCl_2(\mathbf{1})]$ is pseudo-tetrahedral [7] like $[CoCl_2(PPh_3)_2]$ [8]. Furthermore, ligand **1** is unable to force a wide P-M-P angle in its complexes with Cu(I): this angle is only 131.9 (1)° in $[CuCl(\mathbf{1})]$ [5] and 126.0 (1)° in $[CuBr(PPh_3)_2]$ [9].

These results left open the question of the extent to which the presence of ligand **1**, instead of two monodentate phosphines of similar electronic properties, affected the reactivity of its complexes in reactions such as nucleophilic substitution and oxidative-addition. Especially, for square planar complexes of type **2**, the bulky organic *trans*-spanning ring system and the four phenyl groups of ligand **1** might be expected to cause a significant steric hindrance for the attack on the complex by substituting ligands or by oxidants. Dissociative substitution mechanisms for sterically blocked complexes have been described previously [10–14] and could not be excluded in the present case.

The question of the extent of steric blocking and flexibility of ligand **1** became relevant when it was observed that the reaction of $Na_2[PtCl_4]$ with ligand **1** gave *trans*-$[PtCl_2(\mathbf{1})]$ [3] while the addition of HCl to a solution of a Pt(O)-complex containing ligand **1** gave *cis*-$[PtCl_2(\mathbf{1})]$ [15] which contains a highly strained form of ligand **1**. Furthermore, it was observed [16] that the chlorine oxidation of *trans*-$[IrCl(CO)(\mathbf{1})]$ gave only a very small amount of the expected product *trans*-$[IrCl_3(CO)(\mathbf{1})]$ while the complex *trans*-$[IrCl(CO)\{PPh_2(CH_2Ph)\}_2]$, which is electronically similar to *trans*-$[IrCl(CO)(\mathbf{1})]$ [17], oxidized immediately and quantitatively to *trans*-$[IrCl_3(CO)\{PPh_2(CH_2Ph)\}_2]$.

Finally, *Gillie & Stille* [18] have shown that (*i*) the complexes *cis*-$[Pd(Me)_2L_2]$, (L = PPh_3, PPh_2Me; $L_2 = Ph_2PCH_2CH_2PPh_2$) underwent reductive elimination, with formation of ethane, in the presence of coordinating solvents; (*ii*) the complexes *trans*-$[Pd(Me)_2L_2]$, (L = PPh_3, PPh_2Me) underwent reductive elimination in polar solvents as they caused *trans*-to-*cis* isomerization, while (*iii*) the complex *trans*-$[Pd(Me)_2(\mathbf{1})]$ did *not* undergo reductive elimination even at 100° in $(CH_3)_2SO$.

The present kinetic study of substitution reactions on complexes of type **2** containing a derivative of ligand **1** and on the corresponding complexes containing two monodentate phosphines of various steric bulkiness was undertaken to answer some of these questions. Complexes containing ligand **1** or similar phenyl-substituted phosphines are generally insoluble in most solvents. The 3-(trifluormethyl)-phenyl-containing ligands **3** and **4**, however, give MeOH-soluble complexes and were used in the present study. As the bulky substituents on ligands **3** and **4** are expected to cause significant steric hindrance to coordination [19], the reactions

of the corresponding complexes with PEt_3 were also followed for comparison purposes.

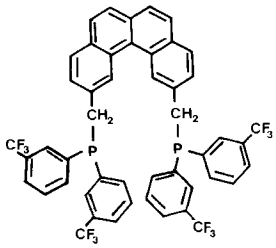

3

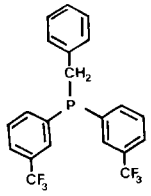

4

To make spectrophotometric detection possible, it is necessary to use an entering or leaving group, which gives sufficiently large absorbance changes on complex formation in the region where the halide complexes have very small molar absorptivities. Pyridine-4-azo-4′-(*N*, *N*-dimethyl)aniline (4-PADA) which coordinates to Pt *via* the pyridine-N-atom, fulfils these requirements *(cf. Fig. 1)*. As for such substitution reactions with steric crowding on the complexes slow reaction rates were expected [10], hydride and methyl were used as *trans*-ligands to obtain reasonable rates within the stopped-flow or rapid conventional time scale. The following reactions were studied:

trans-$[PtHCl(PEt_3)_2]$ + 4-PADA	$\rightleftarrows$	*trans*-$[PtH(4\text{-PADA})(PEt_3)_2]^+ + Cl^-$	(1)
trans-$[PtHCl(\mathbf{4})_2]$ + 4-PADA	$\rightleftarrows$	*trans*-$[PtH(4\text{-PADA})(\mathbf{4})_2]^+ + Cl^-$	(2)
trans-$[PtHCl(\mathbf{3})]$ + 4-PADA	$\rightleftarrows$	*trans*-$[PtH(4\text{-PADA})(\mathbf{3})]^+ + Cl^-$	(3)
trans-$[Pt(Me)Cl(PEt_3)_2]$ + 4-PADA	$\rightleftarrows$	*trans*-$[Pt(Me)(4\text{-PADA})(PEt_3)_2]^+ + Cl^-$	(4)
trans-$[Pt(Me)Cl(\mathbf{4})_2]$ + 4-PADA	$\rightleftarrows$	*trans*-$[Pt(Me)(4\text{-PADA})(\mathbf{4})_2]^+ + Cl^-$	(5)
trans-$[Pt(Me)Cl(\mathbf{3})]$ + 4-PADA	$\rightleftarrows$	*trans*-$[Pt(Me)(4\text{-PADA})(\mathbf{3})]^+ + Cl^-$	(6)
trans-$[PtH(4\text{-PADA})(PEt_3)_2]^+ + I^-$	$\rightarrow$	*trans*-$[PtHI(PEt_3)_2]$ + 4-PADA	(7)
trans-$[PtH(4\text{-PADA})(\mathbf{4})_2]^+ + I^-$	$\rightarrow$	*trans*-$[PtHI(\mathbf{4})_2]$ + 4-PADA	(8)
trans-$[PtH(4\text{-PADA})(\mathbf{3})]^+ + I^-$	$\rightarrow$	*trans*-$[PtHI(\mathbf{3})]$ + 4-PADA	(9)
trans-$[Pt(Me)(4\text{-PADA})(PEt_3)_2]^+ + I^-$	$\rightarrow$	*trans*-$[Pt(Me)I(PEt_3)_2]$ + 4-PADA	(10)
trans-$[Pt(Me)(4\text{-PADA})(\mathbf{4})_2]^+ + I^-$	$\rightarrow$	*trans*-$[Pt(Me)I(\mathbf{4})_2]$ + 4-PADA	(11)
trans-$[Pt(Me)(4\text{-PADA})(\mathbf{3})]^+ + I^-$	$\rightarrow$	*trans*-$[Pt(Me)I(\mathbf{3})]$ + 4-PADA	(12)

2. Experimental. – 2.1. *General.* Melting points (m.p.) were determined using a *Büchi* melting point apparatus and are uncorrected. IR spectra were recorded using a *Beckman IR 4250* spectrometer. ^1H-, $^{31}P\{^1H\}$- and $^{13}C\{^1H\}$-NMR spectra were measured using *Bruker HX-90* and *WM-250* NMR spectrometers. Chemical shifts are in ppm. Those of ^{31}P are relative to external H_3PO_3. A positive sign indicates a resonance to low field of the reference. All *J* values are given in Hz. Elemental analyses of C, H and N were performed by the *Microanalytical Laboratory* and of Cl, P and Pt by the *Analytical Section of Inorganic Chemistry Laboratory of the ETH Zürich.* All synthetic manipulations involving the preparation and use of free phosphines were carried out in a N_2-atmosphere. $[Pt(COD)_2]$ (COD = 1,5-cyclooctadiene) was supplied by *Emser Werke Zürich.*

2.2. *Preparation of Ligands and Complexes.* – *Bis(3-trifluoromethylphenyl)benzylphosphine oxide.* A solution of $(3\text{-}CF_3 \cdot C_6H_4)_2P(O)Li$ was prepared by the addition of 40.4 ml of a 1.83M solution (74 mmol) of BuLi to a stirred solution of 25 g (74 mmol) $(3\text{-}CF_3 \cdot C_6H_4)_2P(O)H$ [20] in 140 ml dry THF which had been cooled to $-40°$. The resulting red solution was stirred for 1 h at r.t., cooled to 0° and treated with a solution of 12.6 g (74 mmol) benzyl bromide in 30 ml THF. After stirring over night at r.t., the solvent was evaporated under reduced pressure, the residue dissolved in $CHCl_3$ and the solution washed with H_2O (3×300 ml). The org. layer was dried over $MgSO_4$ and the solvent evaporated under reduced pressure after filtration. The crude product was purified by recrystallization from benzene/Et_2O and gave 28.3 g (89%) of the colorless crystalline product of m.p. 146°. ^{1}H-NMR ($CDCl_3$): 7.0–8.1 (*m*, 13 H); 3.68 (*d*, $^2J(P,H) = 14$, 2 H). ^{31}P-NMR ($CDCl_3$): 27.6 (*s*). $C_{21}H_{15}F_6OP$ (428.3); found: C, 59.12; H, 3.72%; calc.: C, 58.88; H, 3.53%.

Bis(3-trifluoromethylphenyl)benzylphosphine (**4**). The phosphine oxide was reduced as described by *Vineyard et al.* [21]; 8.4 g (19.6 mmol) $(3\text{-}CF_3 \cdot C_6H_4)_2(CH_2 \cdot C_6H_5)P(O)$ dissolved in 46 ml of anh. acetonitrile and 9.1 ml anh. Et_3N were heated to 70°. At this point 5.8 ml (57.8 mmol) $SiHCl_3$ (freshly distilled over quinoline) were slowly added. The mixture was then kept at 70° for 3 h, cooled to r.t. and treated with 29 ml of 25% NaOH. The org. layer was separated, washed with additional 12 ml of 25% NaOH, and the solvent evaporated under reduced pressure. To the remaining oil 5 ml of MeOH was added and the solution cooled to $-80°$. The pure product, which crystallized out, was filtered off and dried. Yield 7.4 g (91%), m.p. (dec.) $\approx 28°$. ^{1}H-NMR ($CDCl_3$): 6.9–8.0 (*m*, 13 H); 3.44 (*s*, 2 H). ^{31}P-NMR ($CDCl_3$): -9.5 (*s*). $C_{21}H_{15}F_6P$ (412.3); found: C, 61.21; H, 3.77; P, 7.46%; calc.: C, 61.17; H, 3.67; P, 7.51%.

Bis(3-trifluoromethylphenyl)phosphine. 47 g (0.139 mol) $(3\text{-}CF_3 \cdot C_6H_4)_2P(O)H$ [20] was reduced with $SiHCl_3$ as described above. The org. layer was fractionally distilled; 36 g of product (80%) was collected at 77°/0.02 Torr. The IR-, ^{1}H- and ^{31}P-NMR spectra have been reported in [20].

2,11-Bis[bis(3-trifluoromethylphenyl)phosphinomethyl)]benzo[c]phenanthrene (**3**). A red solution of $(3\text{-}CF_3 \cdot C_6H_4)_2PNa$ was prepared by the addition of 8 g (24.8 mmol) $(3\text{-}CF_3 \cdot C_6H_4)PH$ to a stirred solution of 0.58 g (25 mmol) Na in 100 ml anh. liq. NH_3. After 1 h 5.18 g (12.4 mmol) 2,11-bis-(bromomethyl)benzo[*c*]phenanthrene [2] and 20 ml dried Et_2O were added. The solvent was evaporated, the residue dissolved in CH_2Cl_2 and washed repeatedly with H_2O until the washings were neutral. The org. layer was dried over $MgSO_4$, filtered and evaporated under reduced pressure. The crude product was recrystallized from 10 ml MeOH. Yield 8.9 g (89%). The physical data of the pure product thus obtained corresponded to those reported in [20].

Pyridine-4-azo-4'-(N,N-dimethyl)aniline (4-PADA) was prepared as described in [22] but recrystallized from CH_2Cl_2/petrolether (30–60°). Yield 10.3 g (48%), m.p. 210°. UV/VIS (CH_2Cl_2): max. 435 (2.9×10^4) (see also *Fig. 1*). ^{1}H-NMR ($CDCl_3$): 8.50 (*m*, 2 H); 7.92 (*m*, 2 H); 7.64 (*m*, 2 H); 6.75 (*m*, 2 H); 3.12 (*s*, 6 H).

trans-*[PtHCl(PEt$_3$)$_2$]* was prepared as described by *Parshall* [23].

trans-*[Pt(Me)Cl(PEt$_3$)$_2$]* was prepared by displacing COD from *cis*-[Pt(Me)Cl(COD)] [24] with PEt_3 as described in [25] [26]. The reaction was performed in MeOH at r.t. using a 10% excess of phosphine. The product was recrystallized from MeOH/H_2O. Yield 1.1 g (99%). Its ^{1}H- and ^{31}P-NMR parameters agree with those given by *Allen & Pidcock* [27].

trans-*[Pt(Me)Cl* (**3**)*]* was prepared using the method outlined above. The stoichiometric reaction was performed in acetone. The product was recrystallized from hot acetone/MeOH. Yield 8.16 g (98%), m.p. (dec.) $> 265°$. ^{1}H-NMR ($CDCl_3$): 10.56 (*s*, 2 H); 6.9–8.4 (*m*, 24 H); 5.35 (*dt*, $^2J(H,H) = 13.6$, $|^2J(P,H) + {}^4J(P,H)| = 9.7$, $^3J(Pt,H) = 18$, 2 H); 3.83 (*dt*, $^2J(H,H) = 13.6$, $|^2J(P,H) + {}^4J(P,H)| = 8.2$, $^3J(Pt,H) = 53$, 2 H); -0.06 (*t*, $^3J(P,H) = 6$, $^2J(Pt,H) = 80$, 3 H). ^{31}P-NMR ($CDCl_3$): 25.0 (*s*, $^1J(Pt,P) = 3168$). $C_{49}H_{33}ClF_{12}P_2Pt$ (1142.2) found: C, 51.57; H, 2.95; Cl, 3.14; P, 5.47; Pt, 17.10%; calc.: C, 51.52; H, 2.91; Cl, 3.10; P, 5.42; Pt, 17.08%.

trans-*[Pt(Me)Cl* (**4**)$_2$*]*. Also this compound was prepared by the method given above. The reaction was performed in benzene and stoichiometric amounts of the reagents were used. The product crystallized out by adding EtOH to the benzene solution. Yield 2.48 g (95%), m.p. (dec.) $> 183°$. ^{1}H-NMR ($CDCl_3$): 6.9–7.8 (*m*, 26 H); 4.26 (*t*, $|^2J(P,H) + {}^4J(P,H)| = 8$, $^3J(Pt,H) = 27$, 4 H); -0.25 (*t*, $^3J(P,H) = 6$, $^2J(Pt,H) = 79$, 3 H). ^{31}P-NMR ($CDCl_3$): 25.8 (*s*, $^1J(Pt,P) = 3165$). $C_{43}H_{33}ClF_{12}P_2Pt$

(1070.2) found: C, 48.44; H, 3.11; Cl, 3.27; P, 5.70; Pt, 18.42%; calc.: C, 48.26; H, 3.11; Cl, 3.31; P, 5.79; Pt, 18.23%.

trans-*[PtHCl(3)]*. To 2.05 g (2.3 mmol) of **3**, dissolved in 5 ml benzene, 1.50 g (2.2 mmol) *trans*-[PtHCl(PPh_3)$_2$] [28], were added. The pure colorless product crystallized out from the stirred solution. Yield 2.03 g (82%), m.p. (dec.) > 204°. IR (Nujol): 2250–2290 (Pt,H). ^{1}H-NMR ($CDCl_3$): 10.15 (*s*, 2 H); 6.9–8.1 (*m*, 24 H); 4.58 (*t*, $|^2J(P,H)+{}^4J(P,H)| = 8$, $^3J(Pt,H) = 32.4$ H); −15.83 (*t*, $^2J(P,H) = 11$, $^1J(Pt,H) = 1258$, 1 H). ^{31}P-NMR ($CDCl_3$): 27.3 (*s*, $^1J(Pt,P) = 3053$). $C_{48}H_{31}ClF_{12}P_2Pt$ (1128.3) found: C, 51.09; H, 2.67; Cl, 3.20; P, 5.56; Pt, 17.07%; calc.: C, 51.10; H, 2.77; Cl, 3.14; P, 5.49; Pt, 17.30%.

trans-*[PtHCl(4)$_2$]*. 460 mg (1.12 mmol) [Pt(COD)$_2$] and 923 mg (2.24 mmol) of **4** were dissolved in 10 ml toluene at −21° and 11.5 ml 0.1N aq. HCl were slowly added to the stirred solution which was then allowed to warm up to r.t. The org. layer was separated, dried over $MgSO_4$, filtered and the solvent removed under reduced pressure. The oily residue crystallized when stirred with hexane. The product was recrystallized from toluene/hexane. Yield 880 mg (74%), m.p. (dec.) > 116°. IR (Nujol): 2200 (Pt–H). ^{1}H-NMR ($CDCl_3$): 7.0–8.0 (*m*, 26 H); 4.12 (*t*, $|^2J(P,H)+{}^4J(P,H)| = 8$, $^3J(Pt,H) = 33$, 4 H); −16.57 (*t*, $^2J(P,H) = 12$, $^1J(Pt,H) = 1231$, 1 H). ^{31}P-NMR ($CDCl_3$): 27.4 (*s*, $^1J(Pt,P) = 3072$). $C_{42}H_{31}Cl^{\cdot}{}_{12}P_2Pt$ (1056.9) found: C, 47.92; H, 2.98; Cl, 3.39; P, 5.92; Pt, 18.25%; calc.: C, 47.76; H, 2.96; Cl, 3.35; P, 5.86; Pt, 18.46%

trans-*[PtH(4-PADA)(PEt$_3$)$_2$][BF$_4$]* (**5**). A solution of 392 mg (2.0 mmol) $AgBF_4$ in 5 ml acetonitrile was added to 942 mg (2.0 mmol) *trans*-[PtHCl(PEt_3)$_2$] dissolved in 4 ml acetonitrile. After 1 h the AgCl was centrifuged off, the solvent removed under reduced pressure and the residue dissolved in acetone. To this solution 456 mg (2.0 mmol) 4-PADA were added. The solvent was evaporated off and the residue washed with Et_2O (3× 10 ml). The product was recrystallized from acetone/Et_2O. Yield 1.186 g (79%). IR (Nujol): 2205 (Pt–H). UV/VIS (CH_2Cl_2): max. 503 (4.3×10^4). NMR parameters are given in *Section 2.4*. $C_{25}H_{45}BF_4N_4P_2Pt$ (745.5) found: C, 40.52; H, 6.18; N, 7.42; P, 8.36; Pt, 25.88%; calc.: C, 40.28; H, 6.08; N, 7.52; P, 8.31; Pt, 26.17%.

trans-*[PtH(4-PADA)(3)][BF$_4$]* was prepared similarly to **5**. Yield 463 mg (71%). UV/VIS (Ch_2Cl_2): max. 510 (4.0×10^4). IR (Nujol): 2220 (Pt–H). ^{1}H-NMR ([D$_6$]acetone): 10.12 (*s*, 2 H); 6.8–8.5 (*m*, 32 H); 4.87 (*t*, $|^2J(P,H)+{}^4J(P,H)| = 8$, $^3J(Pt,H) = 51$, 4 H); 3.17 (*s*, 6 H); −16.55 (*t*, $^2J(P,H) = 13$, $^1J(Pt,H) = 1016$, 1 H). ^{31}P-NMR ([D$_6$]acetone): 28.2 (*s*, $^1J(Pt,P) = 2950$). $C_{61}H_{45}BF_{16}N_4P_2Pt$ (1405.9) found: C, 52.52; H, 3.42; N, 3.84; P, 4.30; Pt, 13.96%; calc.: C, 52.12; H, 3.23; N, 3.99; P, 4.41; Pt, 13.88%.

trans-*[PtH(4-PADA)(4)$_2$][BF$_4$]* was prepared similarly to **5**. Yield 495 mg (80%). UV/VIS (CH_2Cl_2): max. 505 (4.4×10^4). IR (Nujol): 2220 (Pt–H). ^{1}H-NMR ([D$_6$]acetone): 6.8–8.1 (*m*, 34 H); 4.47 (*t*, $|^2J(P,H)+{}^4J(P,H)| = 8$, $^3J(Pt,H) = 42$, 4 H); 3.18 (*s*, 6 H); −17.51 (*t*, $^2J(P,H) = 12$, $^1J(Pt,H) = 995$, 1 H). ^{31}P-NMR ([D$_6$]acetone): 31.7 (*s*, $^1J(Pt,P) = 3031$). $C_{55}H_{45}BF_{16}N_4P_2Pt$ (1333.8) found: C, 49.61; H, 3.44; N, 4.20; P, 4.64; Pt, 14.91%; calc.: C, 49.53; H, 3.40; N, 4.20; P, 4.64; Pt, 14.63%.

trans-*[Pt(Me)(4-PADA)(PEt$_3$)$_2$][BF$_4$]* was prepared similarly to **5**. Yield 320 mg (82%). UV/VIS (CH_2Cl_2): max. 505 (4.5×10^4). ^{1}H-NMR ([D$_6$]acetone): 8.92 (*m*, $^3J(Pt,H) = 20$, 2 H); 7.95 (*m*, 2 H); 7.90 (*m*, 2 H); 6.92 (*m*, 2 H); 3.20 (*s*, 6 H); 1.70 (*m*, 12 H); 1.12 (*m*, 18 H); 0.49 (*t*, $^3J(P,H) = 7$, $^2J(Pt,H) = 74$, 3 H). ^{31}P-NMR ([D$_6$]acetone): 27.7 (*s*, $^1J(Pt,P) = 2725$). $C_{26}H_{47}BF_4N_4P_2Pt$ (759.5) found: C, 40.94; H, 6.25; N, 7.25; P, 8.15; Pt, 26.23%; calc.: C, 41.12; H, 6.24; N, 7.38; P, 8.16; Pt, 25.69%.

trans-*[Pt(Me)(4-PADA)(3)][BF$_4$]* was prepared as described for **5**. Yield 425 mg (88%). UV/VIS (CH_2Cl_2): max. 510 (4.3×10^4). ^{1}H-NMR (250 MHz, [D$_6$]acetone): 10.48 (*s*, 2 H); 6.5–9.0 (*m*, 30 H); 8.53 (*m*, $^3J(Pt,H) \approx 20$, 2 H); 4.93 (*d, t*, $|^2J(P,H)+{}^4J(P,H)| = 9$, $^2J(H,H) = 15$, 2 H); 4.60 (*d, t*, $|^2J(P,H)+{}^4J(P,H)| = 8$, $^2J(H,H) = 15$, 2 H); 3.14 (*s*, 6 H); 0.94 (*t*, $^3J(P,H) = 7$, $^2J(Pt,H) = 67$, 3 H). ^{31}P-NMR ([D$_6$]acetone): 21.1 (*s*, $^1J(Pt,P) = 3012$). $C_{62}H_{47}BF_{16}N_4P_2Pt$ (1419.9) found: C, 52.71; H, 3.58; N, 3.93; P, 4.24; Pt, 13.70%; calc.: C, 52.45; H, 3.34; N, 3.95; P, 4.36; Pt, 13.74%.

trans-*[Pt(Me)(4-PADA)(4)$_2$][BF$_4$]* was prepared as described for **5**. Yield 476 mg (75%). UV/VIS (CH_2Cl_2): max. 507 (4.2×10^4). ^{1}H-NMR ([D$_6$]acetone): 6.8–8.4 (*m*, 34 H); 4.35 (*t*, $|^2J(P,H)+{}^4J(P,H)| = 8$, $^3J(Pt,H) = 30$, 4 H); 3.17 (*s*, 6 H); 0.44 (*t*, $^3J(P,H) = 7$, $^2J(Pt,H) = 70$, 3 H); ^{31}P-NMR ([D$_6$]acetone): 22.9 (*s*, $^1J(Pt,P) = 3049$). $C_{56}H_{47}BF_{16}N_4P_2Pt$ (1347.9) found: C, 50.18; H, 3.63; N, 4.19; P, 4.55; Pt, 14.25%; calc.: C, 49.90; H, 3.51; N, 4.16; P, 4.60; Pt, 14.47%.

2.3. *Chemicals and Solutions.* Stock solutions of Pt-complexes and ligands were prepared using MeOH and acetone (both *Merck p.a.*) as solvents. Ligand solutions were prepared from LiCl *(Mallinckrodt p.a.)*, $LiCl \cdot H_2O$ *(Merck Suprapur)*, NaI *(Merck Suprapur)*, KI *(Merck p.a.)* and 4-PADA. $LiClO_4 \cdot 3\,H_2O$ *(G. Frederick Smith p.a.)* was used as supporting electrolyte. All solutions had the ionic strength 2.5×10^{-2} M where not otherwise stated.

The compounds *trans*-[PtRCl(**4**)$_2$], *trans*-[PtRCl(**3**)], *trans*-[PtR(4-PADA)(**4**)$_2$][BF_4] and *trans*-[PtR(4-PADA)(**3**)][BF_4] (R = H, Me) are very slightly soluble in MeOH. Thus, stock solutions were prepared by dissolving the solids in a small volume of acetone and subsequently diluting with MeOH. Therefore, the solutions used for the kinetics contained *ca.* 0.1% (*v/v*) acetone. The solutions of the hydride complexes, which undergo slow decomposition, were freshly prepared immediately before starting of a kinetic run.

When *Reactions 1–6* were run at the highest [Cl^-]/[4-PADA] ratios the complexes *trans*-[PtR(4-PADA)L_2] and *trans*-[PtR(4-PADA)(L⌒L)][BF_4] (R = H, Me; L = PEt_3, **4**; L⌒L = **3**) were used as substrates instead of the corresponding chloro-complexes.

2.4. *Coordination of 4-PADA.* The NMR spectra of acetone solutions of compound **5** were recorded using a *Bruker HX-90* instrument. The observed couplings of C(2), C(3) and H–C(2) to ^{195}Pt indicate that in compound **5** 4-PADA is coordinated to the metal *via* the pyridine-N-atom. The following NMR parameters were recorded: ^{1}H-NMR ([D_6]acetone): 8.94 (*m*, ^3J(Pt,H) = 22, 2 H, H–C(2)); 7.90 (*m*, 4 H, H–C(3) and H–C(3′)); 6.90 (*m*, 2 H, H–C(2′)); 3.18 (*s*, 6 H, H_3C–N); 1.8 (*m*, 12 H, H_2C–P); 1.1 (*m*, 18 H, H_3C–CH_2P); – 18.69 (*t*, ^2J(P,H) = 15, ^1J(pt,H) = 1100, 1 H, H–Pt). ^{13}C-NMR ([D_6]acetone): 153.8 (*s*, ^2J(Pt,C) = 16. 2 C, C(2)); 127.4 (*s*, 2 C, C(3′)); 119.3 (*s*, ^3J(Pt,C) = 25, 2 C, C(3)); 112.4 (*s*, 2 C, C(2′)); 159.1, 155.3 and 144.1 (*s*, 3 C, C(1′), C(4) and C(4′)); 40.1 (*s*, 2 C, CH_3–N); 18.0 (*t*, $|^1J(P,C) + {}^3J(P,C)| = 35$, ^2J(Pt,C) = 43, 6 C, CH_2–P); 8.4 (*s*, ^3J(Pt,C) = 29, 6 C, CH_3–CH_2P). ^{31}P-NMR ([D_6]acetone): 20.7 (*s*, ^1J(Pt,P) = 2642).

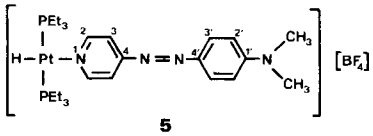

5

2.5. *Kinetics.* All reactions were monitored spectrophotometrically at wavelengths between 360 and 590 nm. *Figure 1* gives an example of the absorbance changes recorded. The halide complexes have very small molar absorptivities in the wavelength regions studied. The temperature was 30.0° in all experiments and the solvent was MeOH (with *ca.* 0.1% (*v/v*) acetone for the complexes containing ligands **3** and **4**).

Slow reactions were started by mixing equal volumes of Pt- and ligand-solutions directly in the thermostated 1-cm cell using thermostated syringes. A *Techtron M 635* spectrophotometer with a *W + W Recorder 1100* was used for detection. Faster reactions were followed using a *Durrum-Gibson* stopped-flow spectrophotometer thermostated at 30°. Transmittance *vs.* time curves were recorded using a *Textronix* storage oscilloscope type *RM 564*. The first-order rate constants were evaluated using a least-squares programme.

All reactions were studied under pseudo-first-order conditions. The concentration of the platinum complexes ranged from 2×10^{-6} to 1.25×10^{-4} M, and the concentration range of ligands was at least ten times larger.

For the *Reactions 1–6* the concentrations of both the entering and leaving ligand were at least 10 times higher than those of the Pt-complex. Series of experiments with a constant ratio [Cl^-]/[4-PADA] were performed.

As a rule, the reactions were recorded for three half-lives and the equilibrium values were obtained by measuring the absorbance after at least 7 half-lives. The kinetic runs were repeated several times. The reproducibility of the rate constants was always better than 10%. *Tables 1* and *2* summarize all experiments.

Further details about experimental procedures are given in [29].

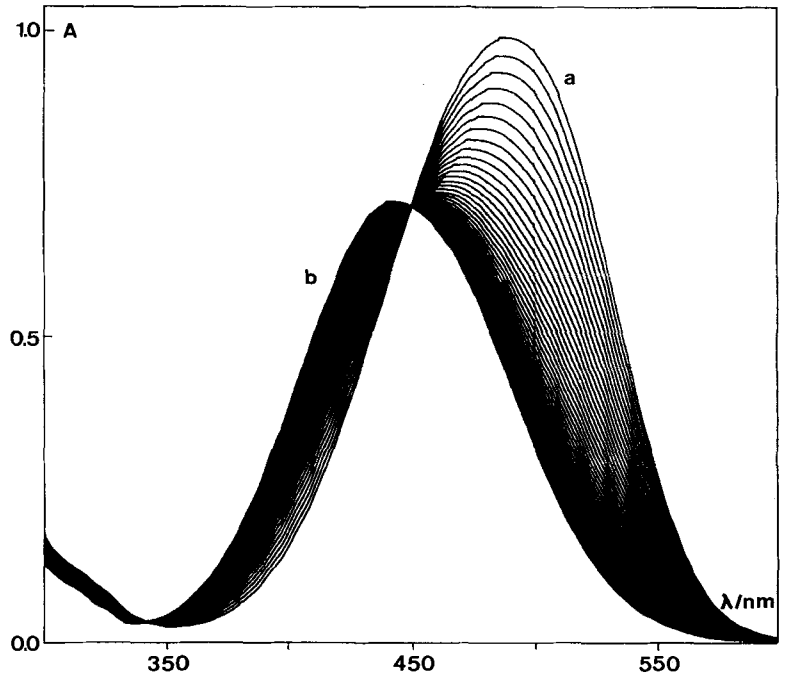

Fig. 1. *Absorbance change for* Reaction 10 *as a function of time.* Curve *a* represents the starting complex *trans*-[Pt(Me)(4-PADA)$(PEt_3)_2$]$^+$ immediately after mixing with excess iodide in MeOH. Curve *b* represents the spectrum at equilibrium. The latter spectrum corresponds to that of free 4-PADA.

Table 1. *Experimental Conditions and Rate Constants for* Reactions 1–6 (ionic strength 2.5×10^{-2} M; 30°)

$[Cl^-]$/[4-PADA]	10^3 [4-PADA]/M	10^5 C_{Pt}/M	λ/nm	$10k_{exp}$/s^{-1}	$[Cl^-]$/[4-PADA]	10^3 [4-PADA]/M	10^5 C_{Pt}/M	λ/nm	$10k_{exp}$/s^{-1}
Reaction 1									
12.5	0.05	0.4	555	0.109	1	0.5	1.25	575	0.280
	0.25	1.0	570	0.293		1.0	1.25	575	0.39
	0.37	1.0	570	0.422		2.5	1.25	575	0.68
	0.50	1.0	572	0.50		3.5	1.25	565	0.93
	0.70	1.0	570	0.71		5.0	1.25	595	1.22
	0.87	1.0	570	0.93	0.1	0.5	0.50	560	1.01
	1.00	1.0	570	1.02		1.4	1.25	575	1.13
	1.25	1.0	570	1.28		3.0	1.25	575	1.45
6.25	1.0	1.25	558	0.53		4.0	1.25	575	1.52
	2.0	1.25	558	1.09		5.0	1.25	575	1.87
	3.0	1.25	558	1.65	0.0625	0.5	0.25	540	1.47
	4.0	1.25	565	2.39		1.5	0.50	565	1.57
	5.0	1.25	565	2.97	0.05	0.5	0.25	540	1.61
5	0.5	1.25	575	0.294		1.0	0.50	555	1.77
	0.8	1.25	575	0.46		1.5	0.75	565	1.85
	2.0	1.25	575	0.99		2.5	1.25	575	2.05
	3.0	1.25	575	1.43		3.5	1.25	570	2.22
	5.0	1.25	575	2.52		5.0	1.25	575	2.47

Table 1 (contd.)

$[Cl^-]$/ [4-PADA]	10^3 [4-PADA]/ M	10^5 C_{Pt}/M	λ/nm	$10k_{exp}$/ s^{-1}
0.01	2.5	0.25	555	4.91
	5.0	0.50	563	5.12
	10.0	1.00	572	6.28
Reaction 2				
12.5	0.05	0.4	555	2.44
	0.25	1.0	568	11.8
	0.37	1.0	575	15.9
	0.50	1.0	570	21.1
	0.70	1.0	562	33.8
	0.87	1.0	567	44
	1.00	1.0	568	51
6.25	1.0	5.0	565	22.6
	2.0	12.5	582	44.1
	3.0	12.5	572	64.1
	4.0	12.5	565	104
	5.0	12.5	571	123
0.05	0.5	0.25	545	2.14
	1.5	0.75	560	4.6
	2.5	1.0	577	7.5
	3.5	1.0	575	10.6
	5.0	1.0	575	14.0
0.01	2.5	0.25	555	8.7
	5.0	0.5	570	13.8
Reaction 3				
12.5	0.05	0.4	561	0.97
	0.25	1.0	568	5.92
	0.37	1.0	567	9.29
	0.50	1.0	575	11.9
	0.70	1.0	565	15.7
	0.87	1.0	567	21.2
	1.00	1.0	565	22.7
	1.25	1.0	577	30.3
6.25	1.0	5.0	560	11.3
	2.0	12.5	557	23.0
	3.0	12.5	555	35.6
	4.0	12.5	560	44.8
	5.0	12.5	562	67.5
5	0.5	1.25	538	4.6
	0.8	8.75	575	5.8
	2.0	12.5	575	21.2
	3.0	12.5	575	34.2
0.0625	0.5	0.25	545	0.294
	1.5	0.75	570	0.94
0.05	0.5	0.25	545	0.37
	1.5	0.75	570	0.93
	2.5	1.25	577	1.38
	3.5	1.25	577	1.95
	5.0	12.5	575	2.53
0.01	2.5	0.25	555	1.19
	5.0	0.5	565	2.33
	10.0	1.0	572	4.07
Reaction 4				
10	0.25	1.25	550	0.57×10^{-4}
	0.50	1.25	550	0.79
	1.25	1.25	550	1.53
	2.50	1.25	550	2.84
0.1	0.5	0.50	550	13.9×10^{-4}
	2.5	1.25	550	18.0
	5.0	1.25	560	22.6
0.02	2.5	0.5	550	58.7×10^{-4}
	5.0	1.0	560	60.2
Reaction 5				
10	0.25	1.25	550	1.49×10^{-3}
	1.25	1.25	550	7.3
	2.50	1.25	550	16.1
0.1	0.5	0.5	550	0.46×10^{-3}
	2.5	1.25	550	1.57
	5.0	1.25	560	2.80
0.02	2.5	0.5	550	2.03×10^{-3}
	5.0	1.0	560	3.37
Reaction 6				
10	0.25	1.25	550	0.93×10^{-4}
	1.25	1.25	550	5.2
	2.50	1.25	550	11.1
0.1	0.5	0.5	550	0.41×10^{-4}
	2.5	1.25	550	1.54
	5.0	1.25	560	3.01
0.02	2.5	0.5	550	1.65×10^{-4}
	5.0	1.0	560	2.96

Table 2. *Experimental Conditions and Rate Constants for* Reactions 7–12 (ionic strength 2.5×10^{-2} M, unless otherwise stated; 30°)

10^3 [I$^-$]/M	10^5 C_{Pt}/M	λ/nm	k_{exp}/s^{-1}
Reaction 7			
0.5	1.0	570	1.85
2.5			10.8
5.0			20.6
12.5			49.4
Reaction 8			
0.05	1.0	550	15.9
0.10			33.6
0.15			51.9
0.25			81.7
Reaction 9			
0.0125	0.2	510	24
0.0250	0.2		56
0.050	0.5		111
Reaction 10			
2.5	1.25	510	0.181×10^{-2}
12.5			1.03
25.0			1.68
Reaction 11			
2.5	2.0	360–590	1.70[a])
			0.83
5.0			2.92[b])
			1.64[c])
10.0			4.8[d])
			3.3
15.0			6.4[e])
			5.1[c])
20.0			7.7[f])
			6.9[c])
25.0			8.4
Reaction 12			
2.5	2.0	360–590	0.034
10.0			0.139
15.0			0.220
20.0			0.292
25.0			0.36

Ionic strengths: [a]) 2.5×10^{-3} M. [b]) 5.0×10^{-3} M. [c]) Value calculated using *Equation 19*. [d]) 10.0×10^{-3} M. [e]) 15×10^{-3} M. [f]) 20×10^{-3} M.

3. Calculations and Results. – 3.1. *Rate Expressions.* If an associative mechanism for the solvent path is assumed, the *Overall Reactions 1–6* can be described by the *Scheme*, where X (Cl^-) is the leaving and Y (4-PADA) the entering ligand and S denotes a solvent molecule (MeOH). For excess X and Y compared to substrate complex, the *Scheme* gives the pseudo-first-order rate constant, k_{exp}, of *Equation 13*, if the solvento intermediate $[PtRSL]^+$ is assumed to be present in steady-state concentration. Further details are given elsewhere [30]. The first term of *Equation 13*

Scheme

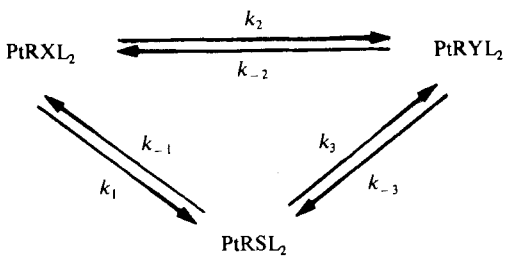

$$k_{exp} = \frac{k_1 + \dfrac{k_1 k_{-2}[X]}{k_2[Y]}}{1 + \dfrac{k_{-1}[X]}{k_3[Y]}} + k_{-2}[X] + k_2[Y] \qquad (13)$$

describes the contribution from the solvent path, while the second and third arise from the direct reaction. *Equation 13* will have the same form if the reaction described by k_1, k_{-1}, k_3, k_{-3} takes place *via* an intermediate of coordination number lower than four.

3.2. *Calculation of Rate Constants. Reactions 1–6* were studied using constant ratios $[Cl^-]/[4\text{-PADA}]$ and the rate constants were evaluated from *Equation 13* in the form *14* using linear regression. *Figure 2* shows plots of k_{exp} *vs.* [4-PADA] for constant ratios $[Cl^-]/[4\text{-PADA}]$ which conform to *Equation 14*. Thus, it is obvious that both the direct nucleophilic substitution of chloride by 4-PADA, described by the rate constants k_2 and k_{-2}, and the reaction *via* an intermediate described

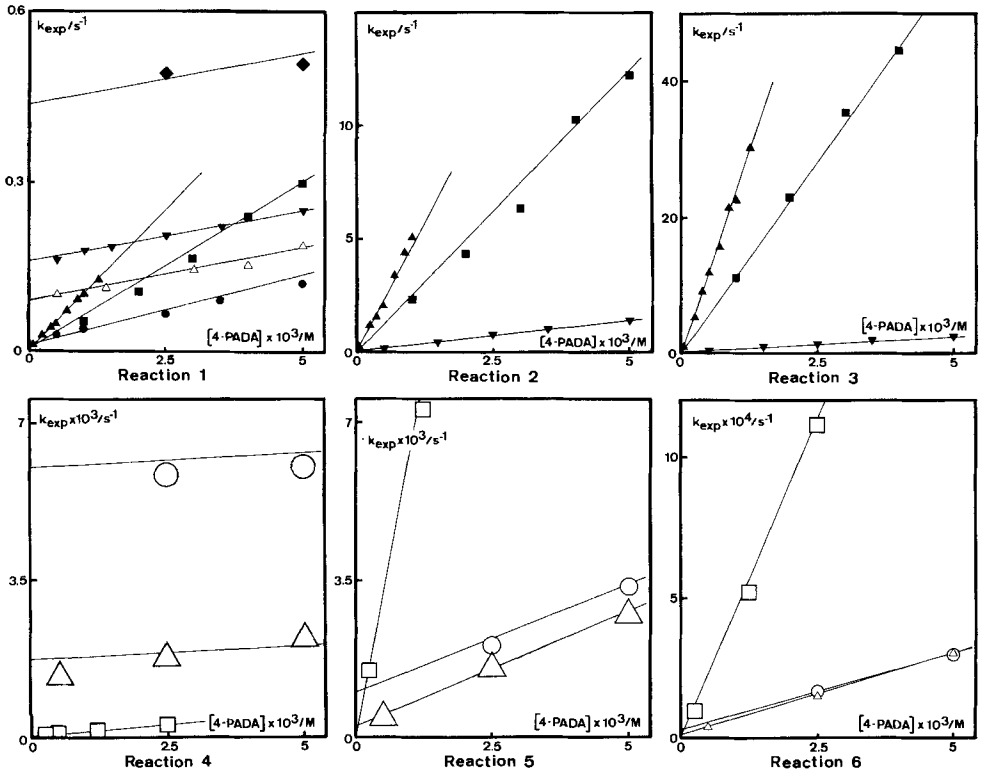

Fig. 2. *Plots of* k_{exp} vs. *[4-PADA] for* Reactions 1–6. The ratios $[Cl^-]/[4\text{-PADA}]$ were 12.5/1 (▲), 10/1 (□), 6.25/1 (■), 1/1 (●), 1/10 (△), 1/20 (▼), 1/50 (○), and 1/100 (◆). The straight lines were calculated from *Eqn. 14* using the final rate constants in *Table 3*. For clarity, some series of experiments have been excluded.

$$k_{exp} = \underbrace{\frac{k_1 + \frac{k_1 k_{-2}[Cl^-]}{k_2[4\text{-PADA}]}}{1 + \frac{k_{-1}[Cl^-]}{k_3[4\text{-PADA}]}}}_{k_I} + \underbrace{(k_{-2}\frac{[Cl^-]}{[4\text{-PADA}]} + k_2)[4\text{-PADA}]}_{k_{SL}} \quad (14)$$

by the rate constants k_1, k_{-1}, k_3 and k_{-3} contribute to the over-all reaction for these complexes. The relative contributions of the two paths depend on the experimental conditions used. For those used here, the contributions from the k_1, k_{-1}, k_3, k_{-3} - path are small for *Reactions 2, 3* and *6*, whereas it is predominant for *Reaction 4*. In no case, however, can one of the two paths be excluded.

It is also likely that the reaction described by the rate constants k_1, k_{-1}, k_3 and k_{-3} takes place *via* a solvento intermediate and not by a dissociative process. Separate experiments using the solvento compounds *trans*-[Pt(Me)(MeOH)(**4**)$_2$]-[BF_4] and *trans*-[Pt(Me)(MeOH)(**3**)][BF_4] as substrate complexes for reactions with 4-PADA were not very reproducible because the MeOH-complexes could not be obtained in an analytically pure state. However, these experiments showed unequivocally that the MeOH-complexes react with 4-PADA about 1000 times faster than the corresponding chloro-complexes. Thus, the condition for steady-state treatment giving *Equation 13* is fulfilled.

Plots like those of *Figure 2* gave k_{SL} as slopes and k_I as intercepts, according to *Equation 14*. Plots of k_{SL} *vs.* $[Cl^-]/[4\text{-PADA}]$ according to *Equation 15* gave k_{-2} and k_2. The known values of k_2 and k_{-2} and the intercepts k_I of *Equation 14*

$$k_{SL} = k_2 + k_{-2}[Cl^-]/[4\text{-PADA}] \quad (15)$$

were then used to calculate k_1 from *Equation 16*.

$$\frac{1 + \frac{k_{-2}[Cl^-]}{k_2[4\text{-PADA}]}}{k_I} = \frac{1}{k_1} + \frac{k_{-1}[Cl^-]}{k_3 k_1[4\text{-PADA}]} \quad (16)$$

Using k_1, the slope of this function also gives a value of the ratio k_{-1}/k_3. Finally, k_{-3} was obtained from *Equation 17*.

$$K = \frac{k_2}{k_{-2}} = \frac{k_1 k_3}{k_{-1} k_{-3}} \quad (17)$$

For *Reactions 7–12* the processes described by k_1, k_{-1}, k_2, k_3 and k_{-3} in the *Scheme* were negligible in the concentration ranges studied. For X = I^-, *Equation 13* then reduces to *18*, which directly gives k_{-2} from plots of k_{exp} *vs.* $[I^-]$. For constant

$$k_{exp} = k_{-2}[I^-] \quad (18)$$

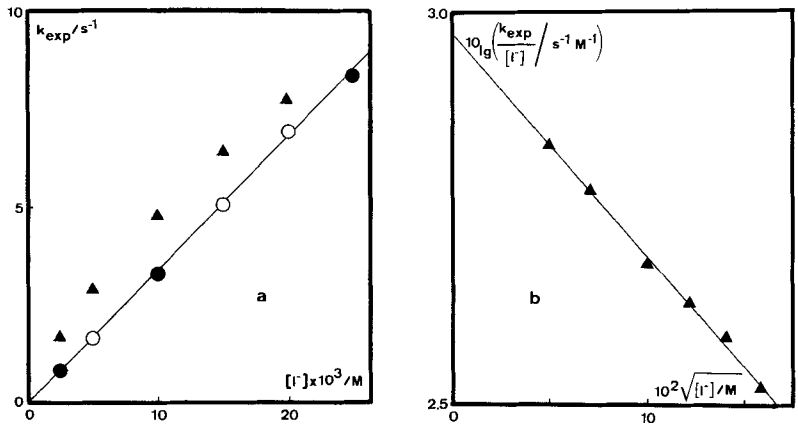

Fig. 3. *Rate constants for* Reaction 11. *a)* Observed rate constants *vs.* iodide concentration. ▲: denotes expts. at various ionic strengths according to *Table 2*, ○: values recalculated to 2.5×10^{-2}M ionic strengths from *Eqn. 19* and ●: values measured at that ionic strength. *b)* Plot according to *Eqn. 19.*

ionic strength, these plots were strictly linear for all reactions. *Figure 3a* shows an example for *Reaction 11.*

Table 3 gives all rate constants. It also contains the equilibrium constants K for *Reactions 1* to *6* calculated from *Equation 17.*

3.3. *Ionic Strength Dependence.* Some of the experiments with varying ionic strengths were performed for *Reaction 11* (see *Table 2* and *Fig. 3*). The plot in *Figure 3b* is linear in agreement with the *Brønsted-Bjerrum Equation 19.*

$$^{10}lg\,(k_{exp}/[I^-]) = {}^{10}lg\,(k_{exp}/[I^-])_0 + 2\,Z_A Z_B a\sqrt{\mu} \qquad (19)$$

The slope of -2.85 is in accordance with a bimolecular reaction between two oppositely charged ions [31] [32]. The theoretical slope for MeOH at 30° is -3.50. Some of the rate constants were then recalculated to $\mu = 2.5\times10^{-2}$M. The complete set now gave a strictly linear k_{exp} *vs.* $[I^-]$ plot, see *Figure 3a.*

4. Discussion. – Substitution reactions of the sterically hindered complex $[PtCl(Et_4dien)]^+$ [$Et_4dien = (Et_2NCH_2CH_2)_2NH$] are much slower than those of $[PtCl(dien)]^+$ [$dien = (H_2NCH_2CH_2)_2NH$] and are practically independent of the concentrations of the entering ligands in the concentration ranges studied [10] [33]. It has been suggested that the usual associative reaction with the entering nucleophiles is suppressed by the steric hindrance of the Et_4dien-ligand in favor of a dissociative process [33].

The substitution of chloride by pyridine in *trans*-$[PtRCl(PEt_3)_2]$ (R = phenyl, *o*-tolyl or mesityl) takes place mainly *via* the solvento intermediates *trans*-$[PtR(MeOH)(PEt_3)_2]^+$, whereas the direct reaction *via* the k_2-path is not very important [12] [13]. On the other hand, the reaction between *trans*-$[PtRCl(PEt_3)_2]$ (R = Me or Et) and various nucleophiles displays the usual two-term rate expressions and a normal dependence of the rate on the nature of the entering group [34]. The steric hindrance in the PEt_3-complexes, therefore, does not seem to be very

Table 3. *Rate Constants and Equilibrium Constants for* Reactions 1–6 (ionic strength 2.5×10^{-2} M; 30°)

Entering group →			MeOH	4-PADA	Cl^-	I^-	MeOH	Cl^-/4-PADA	Cl^-
Leaving group →			Cl^-	Cl^-	4-PADA	4-PADA	4-PADA	MeOH	4-PADA
Reaction	*trans*-Ligand	P-Ligand	k_1/s^{-1}	$k_2/M^{-1}\,s^{-1}$	$k_{-2}/M^{-1}\,s^{-1}$	$k_{-2}/M^{-1}\,s^{-1}$	k_{-3}/s^{-1}	k_{-1}/k_3	$K=k_2/k_{-2}$
1	H	PEt_3	$(7.8\pm1.7)\times10^{-1}$	$(1.83\pm0.06)\times10^{1}$	(6.6 ± 0.7)	–	$(3.5\pm0.1)\times10^{-3}$	80	2.8 ± 0.4
2	H	**4**	$(2\pm8)\times10^{-1}$	$(2.51\pm0.03)\times10^{2}$	$(3.6\pm0.3)\times10^{2}$	–	$(7\pm9)\times10^{-3}$	50	0.69 ± 0.09
3	H	**3**	$(5\pm7)\times10^{-1}$	$(3.61\pm0.10)\times10^{2}$	$(1.9\pm0.4)\times10^{3}$	–	$(5\pm2)\times10^{-2}$	50	0.19 ± 0.05
4	Me	PEt_3	$(1.9\pm0.8)\times10^{-2}$	$(6.0\pm1.0)\times10^{-2}$	$(4.1\pm0.9)\times10^{-3}$	–	$(1.2\pm0.6)\times10^{-5}$	100	15 ± 6
5	Me	**4**	$(9\pm12)\times10^{-3}$	$(4.6\pm1.2)\times10^{-1}$	$(6\pm2)\times10^{-1}$	–	$(3\pm4)\times10^{-5}$	400	0.8 ± 0.4
6	Me	**3**	$(4\pm8)\times10^{-5}$	$(5.4\pm0.7)\times10^{-2}$	$(4.0\pm0.5)\times10^{-2}$	–	$(1\pm2)\times10^{-6}$	20	1.4 ± 0.4
7	H	PEt_3	–	–	–	$(3.9\pm0.2)\times10^{3}$	–	–	–
8	H	**4**	–	–	–	$(3.4\pm0.4)\times10^{5}$	–	–	–
9	H	**3**	–	–	–	$(2.3\pm0.3)\times10^{6}$	–	–	–
10	Me	PEt_3	–	–	–	$(6.6\pm1.2)\times10^{-1}$	–	–	–
11	Me	**4**	–	–	–	$(3.4\pm0.2)\times10^{2}$	–	–	–
12	Me	**3**	–	–	–	$(1.47\pm0.06)\times10^{1}$	–	–	–

significant, *cf.* also [19]. The pressure dependence of reactions of this type supports an associative mechanism both for the k_1- and k_2-paths [14].

It might be expected in the present case that an eventual increasing steric hindrance in the series *trans*-[PtRX(PEt_3)$_2$] < *trans*-[PtRX(**4**)$_2$] < *trans*-[PtRX(**3**)] (R = H, Me; X = Cl^-, I^-, 4-PADA) should favor a reaction *via* a solvento intermediate or even a dissociative process for the complexes of ligands **4** and **3** compared to those of PEt_3. That should be displayed in the kinetics as a preference for the path described by k_1, k_{-1}, k_3, and k_{-3} compared to the direct k_2, k_{-2}-path.

This, however, is contrary to what is observed. The k_1- and k_2-paths are of about equal importance for the PEt_3-complexes, in accordance with the previous study by *Belluco et al.* [34], *cf. Reactions 1* and *4*. For the complexes with ligands **3** and **4**, on the other hand, the direct substitution *via* the k_2-path is predominant, and the contribution from the k_1-path is very small and even difficult to determine experimentally in some cases (see *Table 3* and *Fig. 2*). Thus, the steric blocking of ligands **3** and **4** is obviously not sufficient to hinder the attack on the complex by an entering nucleophile.

One additional reason for the small contributions by the k_1-path in the reactions of the complexes with **3** and **4** might be that the aromatic ring systems of these ligands hinder an efficient solvation of these complexes compared to those of PEt_3. This is paralleled by a large difference in solubility between the two groups of complexes.

Comparison of the rate constants within the various series of complexes lead to a similar conclusion (see *Table 3*). The rate constants k_2, k_{-2}, and k_{-3} for the hydride complexes increase in the order *trans*-[PtHX(PEt_3)$_2$] < *trans*-[PtHX(**4**)$_2$] < *trans*-[PtHX(**3**)] (X = Cl^-, 4-PADA) contrary to what should be expected if there were an increase of steric hindrance in the series.

Similarly, for the methyl series, *trans*-[Pt(Me)X(L_2 or $\widehat{L\,L}$)], the PEt_3-complexes normally react more slowly than the complexes with ligand **4**. However, all rate constants decrease about one order of magnitude, when the phosphine ligands are changed from two molecules of **4** to one of **3**, which is bidentate. One explanation for this decrease might be that the methyl group hinders the flexibility of the *trans*-spanning ligand by interaction with the hydrocarbon moiety of **3**, thereby increasing the steric hindrance exerted by **3**. The small hydride ligand should not be capable of that sort of interaction. Molecular models support this interpretation. Moreover, the ^{1}H-NMR spectrum of the hydride complexes of **1** and **3** show four equivalent CH_2-protons, whereas there are four different signals for the corresponding methyl complexes. This shows that there is a dynamic behavior of the *trans*-spanning ligand **3** in the hydride complexes, which is at least partly frozen in the methyl analogs. This behavior has been discussed in [1].

The above data indicate that the observed inhibition of olefin insertion reactions at platinum-hydride complexes containing the *trans*-spanning ligand **1** compared to those containing two monodentate phosphines [35] is unlikely to be due to a slow substitution step.

This work was supported by the *Swiss National Science Foundation* and by the *Swedish Natural Science Research Council*. *L. I. E.* wants to thank the ETH for financial support of sabbatical leave.

REFERENCES

[1] *P. N. Kapoor, P. S. Pregosin & L. M. Venanzi,* Helv. Chim. Acta *65*, 654 (1982) and ref. quoted therein.
[2] *N. J. DeStefano, D. K. Johnson, R. M. Lane & L. M. Venanzi,* Helv. Chim. Acta *59*, 2674 (1976).
[3] *N. J. DeStefano, D. K. Johnson & L. M. Venanzi,* Helv. Chim. Acta *59*, 2683 (1976).
[4] *M. C. Browning, J. R. Mellor, D. J. Morgan, S. A. J. Pratt, L. E. Sutton & L. M. Venanzi,* J. Chem. Soc. *1962*, 693.
[5] *M. Barrow, H. B. Bürgi, D. K. Johnson & L. M. Venanzi,* J. Am. Chem. Soc. *98*, 2356 (1976).
[6] *N. C. Baenziger, K. M. Dittemore & J. R. Doyle,* Inorg. Chem. *13,* 805 (1974).
[7] *L. M. Venanzi,* Pure Appl. Chem. *52,* 1117 (1980) and ref. quoted therein.
[8] *W. De W. Horrocks & E. S. Greenberg,* Inorg. Chem. *10*, 2190 (1971) and ref. quoted therein.
[9] *P. H. Davis, R. L. Belford & I. C. Paul,* Inorg. Chem. *12*, 213 (1973).
[10] *F. Basolo & R. G. Pearson,* Mechanisms of Inorganic Reactions, 2nd Ed., Wiley 1967, see Ch. 5.
[11] *W. H. Baddley & F. Basolo,* J. Am. Chem. Soc. *86*, 2075 (1964).
[12] *V. Ricevuto, R. Romeo & M. Trozzi,* J. Chem. Soc., Dalton Trans. *1972*, 1857.
[13] *G. Faraone, V. Ricevuto, R. Romeo & M. Trozzi,* J. Chem. Soc., Dalton Trans. *1974*, 1377.
[14] *R. van Eldik, D. A. Palmer & H. Kelm,* Inorg. Chem. *18*, 572 (1979) and ref. quoted therein.
[15] *G. Bracher, D. M. Grove, L. M. Venanzi, F. Bachechi, P. Mura & L. Zambonelli,* Helv. Chim. Acta *63*, 2519 (1980).
[16] *E. Baumgartner, F. J. S. Reed, L. M. Venanzi, F. Bachechi & L. Zambonelli,* to be published. See also *E. Baumgartner,* ETH Dissertation Nr. 6605, 1980.
[17] *F. J. S. Reed & L. M. Venanzi,* Helv. Chim. Acta *60*, 2804 (1977).
[18] *A. Gillie & J. K. Stille,* J. Am. Chem. Soc. *102*, 4933 (1980).
[19] *C. A. Tolman,* Chem. Revs. *77*, 313 (1977).
[20] *P. N. Kapoor & L. M. Venanzi,* Helv. Chim. Acta *60*, 2824 (1977).
[21] *B. D. Vineyard, W. S. Knowles, M. H. Sabacky, G. L. Bachman & D. J. Weinkauff,* J. Am. Chem. Soc. *99*, 5946 (1977).
[22] *R. W. Faessinger & E. V. Brown,* Trans. Kentucky Acad. Sci. *24*, 106 (1963) [Chem. Abstr. *60*, 14465g (1964)].
[23] *G. W. Parshall,* Inorganic Syntheses, Mc Graw Hill *12*, 28 (1970).
[24] *H. C. Clark & L. E. Manzer,* J. Organomet. Chem. *59*, 411 (1973).
[25] *C. R. Kistner, J. H. Hutchinson, J. R. Doyle & J. C. Storlie,* Inorg. Chem. *2*, 1255 (1963).
[26] *H. D. Empsall, E. M. Hyde, E. Mentzer & B. L. Shaw,* J. Chem. Soc., Dalton Trans. *1977*, 2285.
[27] *F. H. Allen & A. Pidcock,* J. Chem. Soc. (A) *1968*, 2700.
[28] *J. C. Bailar & H. Itatani,* Inorg. Chem. *4*, 1618 (1965).
[29] *B. Kellenberger,* ETH Dissertation Nr. 7057, 1982.
[30] *L. I. Elding & A.-B. Gröning,* Inorg. Chim. Acta *38*, 59 (1980).
[31] *J. N. Brønsted,* Z. Phys. Chem. *102*, 169 (1922).
[32] *N. Bjerrum,* Z. Phys. Chem. *108*, 82 (1924).
[33] *C. H. Langford & H. B. Gray,* 'Ligand Substitution Processes', W. A. Benjamin, New York 1965, p. 31–33, and ref. quoted therein.
[34] *U. Belluco, M. Graziani & P. Rigo,* Inorg. Chem. *5*, 1123 (1966).
[35] *G. Bracher,* ETH Dissertation Nr. 6439, 1979.